INTERNATIONAL JOURNAL FOR NUMERICAL METHODS IN FLUIDS
Int. J. Numer. Meth. Fluids 2006; **51**:221–233
Published online 17 November 2005 in Wiley InterScience (www.interscience.wiley.com). DOI: 10.1002/fld.1122

Third-order-accurate semi-implicit Runge–Kutta scheme for incompressible Navier–Stokes equations

Nikolay Nikitin*,†

Institute of Mechanics of Moscow State University, 117192 Michurinsky pr. 1, Moscow, Russian Federation

SUMMARY

A semi-implicit three-step Runge–Kutta scheme for the unsteady incompressible Navier–Stokes equations with third-order accuracy in time is presented. The higher order of accuracy as compared to the existing semi-implicit Runge–Kutta schemes is achieved due to one additional inversion of the implicit operator $I - \tau\gamma L$, which requires inversion of tridiagonal matrices when using approximate factorization method. No additional solution of the pressure-Poisson equation or evaluation of Navier–Stokes operator is needed. The scheme is supplied with a local error estimation and time-step control algorithm. The temporal third-order accuracy of the scheme is proved analytically and ascertained by analysing both local and global errors in a numerical example. Copyright © 2005 John Wiley & Sons, Ltd.

KEY WORDS: Navier–Stokes equations; semi-implicit Runge–Kutta method; third-order accuracy

1. INTRODUCTION

Spatial discretization of the incompressible Navier–Stokes equations with sufficiently fine resolution leads to stiff problems and requires implicit methods for time advancement. Fully implicit methods produce a set of nonlinear coupled equations for the flow variables on the new time level, and are usually prohibitively costly for long-term calculations, such as turbulent flow simulations. Semi-implicit methods, in which only a part of the Navier–Stokes operator is treated implicitly, present a reasonable compromise for this class of flows. In fact, the majority of direct and large eddy simulations to date have used semi-implicit time-advancement methods. In wall-bounded flow simulations only the linear viscous term of the Navier–Stokes equations is usually treated implicitly, and the corresponding set of linear equations is solved effectively with the help of an approximate factorization technique.

*Correspondence to: N. Nikitin, Institute of Mechanics of Moscow State University, 117192, Michurinsky pr. 1, Moscow, Russia.
†E-mail: nta@rsuh.ru

Contract/grant sponsor: Russian Foundation for Basic Research; contract/grant number: 05-01-00607

Received 11 April 2005
Revised 14 September 2005
Accepted 21 September 2005

One of the popular schemes was proposed in Reference [1]. It consists of a second-order-explicit Adams–Bashforth method for the convective terms and a second-order-implicit Crank–Nicolson method for the viscous term. The Adams–Bashforth method, as well as first- and second-order accurate Runge–Kutta methods, is unconditionally unstable for a pure convection equation. However, the instability is weak, and the method usually works for CFL numbers less than 1.0 in the presence of a viscous term. Third-order accurate Runge–Kutta methods seem more suitable for convective terms because of their stability. Slightly different semi-implicit schemes based on a third-order accurate low-storage Runge–Kutta method were presented in References [2–4]. These are the three-step schemes, which require three times more operations to advance to a new time level compared with the scheme of Reference [1]. However, due to high accuracy and stability they are often preferably compared with the Adams–Bashforth-based schemes.

The previously mentioned Runge–Kutta-based schemes use second-order accurate implicit methods for the viscous term, thus, their overall accuracy is second order in time. Apparently, it is impossible to achieve a third-order accuracy within a classical three-step semi-implicit Runge–Kutta method, each step of which consists of the three substeps: (a) evaluation of the convective and viscous terms of the Navier–Stokes equations for a given velocity field, (b) solution of a linear system connected with the implicit terms, (c) solution of a Poisson equation for the pressure (or pseudo-pressure).

In this paper, we present a third-order accurate semi-implicit Runge–Kutta scheme for the Navier–Stokes equations. The higher order of accuracy is achieved due to one extra substep (b). Thus, our scheme may be referred as $3\frac{1}{3}$-step scheme. Note that among the three substeps, solution of the Poisson equation is usually the most time consuming substep except in the case of a spectral spatial discretization. On the contrary, evaluation of the nonlinear convective terms in substep (a) is the most expensive for spectral methods. Regarding substep (b), it is a relatively inexpensive substep both in spectral and finite-difference methods when using approximate factorization technique. Thus, the overall overhead of our scheme is similar to that of the classical one.

The scheme is supplied with a built-in local accuracy estimation and time-step control algorithm. The idea of the time-step control algorithm is not novel. It was first utilized in semi-implicit Runge–Kutta schemes for the Navier–Stokes equations in References [5, 6]. Being extensively exploiting for a period of about 10 years it proved itself to be efficient and convenient, especially for flows with variations in characteristic time scales, for instance, in simulations of laminar–turbulent transition.

One of the difficulties in constructing high-order-accurate implicit time integration schemes for the Navier–Stokes equations is the so-called *pressure problem*. It arises because the equations for the velocity and the pressure are a coupled system with the incompressibility condition. Nearly all numerical schemes for solving Navier–Stokes equations in terms of primitive variables use a *fractional step approach* in which the auxiliary velocity field is at first computed by ignoring the incompressibility constraint and then projected onto a divergence-free field. The determination of boundary conditions for the auxiliary velocity field- and pressure-related quantities has been a subject of considerable discussion in the literature over many years (see Reference [7] and references therein). We construct our scheme in terms of the spatially discretized Navier–Stokes equations. Following this approach [8, 9], no boundary conditions for the auxiliary velocity fields are needed. In our scheme only the final velocity field at each complete time step satisfies a discrete continuity equation exactly, while the

velocities on the intermediate time levels are divergence-free only to within a certain truncation error. Such a trick leads to a relatively simple solution to the pressure problem while retaining a desired order of accuracy.

2. SEMI-IMPLICIT THIRD ORDER ACCURATE RUNGE–KUTTA METHOD

In this section, we construct a semi-implicit third-order accurate Runge–Kutta method for a system of ordinary differential equations

$$\frac{\mathrm{d}w}{\mathrm{d}t} = F(t, w) \tag{1}$$

where $w(t)$ is an unknown vector function, t is an independent variable which will be referred as *time*, and F is a nonlinear operator. We assume that all necessary conditions for existence of sufficiently smooth solution $w(t)$ are satisfied. A semi-implicit method to advance from w_n at time t_n to w_{n+1} at time $t_{n+1} = t_n + \tau$ is based on the following explicit third-order accurate Runge–Kutta method:

$$\frac{w' - w_n}{\tau} = \frac{2}{3}F_n \tag{2}$$

$$\frac{w'' - w_n}{\tau} = \frac{1}{3}F_n + \frac{1}{3}F' \tag{3}$$

$$\frac{w_{n+1} - w_n}{\tau} = \frac{1}{4}F_n + \frac{3}{4}F'' \tag{4}$$

Here $F_n \equiv F(t_n, w_n)$, $F' \equiv F(t_n + 2\tau/3, w')$, and $F'' \equiv F(t_n + 2\tau/3, w'')$. This particular method is selected from a 2-parameter family of the third-order accurate Runge–Kutta methods according to the following requirements. First, the third step of the method (4) does not include F'. This is essential for the following construction of the semi-implicit scheme. Second, the method has the coincident abscissas (F' and F'' are evaluated for the same time moment $t_n + 2\tau/3$), which will be convenient for the Navier–Stokes equations.

The semi-implicit scheme is constructed by perturbing (2)–(4) taking into account the following relations:

$$\begin{aligned} w' &= w(t_n + 2\tau/3) + O(\tau^2) \\ w'' &= w(t_n + 2\tau/3) + O(\tau^3) \\ w_{n+1} &= w(t_{n+1}) + O(\tau^4) \end{aligned} \tag{5}$$

Let L be a linear operator (some approximation to the Jacobian $\partial F/\partial w$) and γ be a positive number. Consider the following implicit scheme:

$$\frac{w' - w_n}{\tau} = \frac{2}{3}F_n + \gamma L(w' - w_n) \tag{6}$$

$$\frac{w'' - w_n}{\tau} = \frac{1}{3}F_n + \frac{1}{3}F' + \gamma L(w'' - w') \tag{7}$$

$$\frac{w_{n+1} - w_n}{\tau} = \frac{1}{4}F_n + \frac{3}{4}F'' + \gamma L(w_{n+1} - \tilde{w}_{n+1}) \tag{8}$$

where $\tilde{w}_{n+1}$ is some $O(\tau^2)$ approximation to $w(t_{n+1})$ (i.e. $\tilde{w}_{n+1} = w(t_{n+1}) + O(\tau^3)$). It is easy to see, that the right-hand side (rhs) of (6) is a $O(\tau)$ perturbation to the rhs of (2), which leads to a $O(\tau^2)$ variation in w' and in F'. Then, the rhs of (7) is a $O(\tau^2)$ perturbation to the rhs of (3), which leads to a $O(\tau^3)$ variations in w'' and in F''. At last, the rhs of (8) is a $O(\tau^3)$ perturbation to the rhs of (4), causing a $O(\tau^4)$ variation in w_{n+1}. Thus, the local error of the scheme $w_{n+1} - w(t_{n+1})$ is still $O(\tau^4)$, so that the scheme retains the third order of accuracy. Note that the absence of F' in the rhs of (8) is a necessary condition for this.

The problem is that $\tilde{w}_{n+1}$, the $O(\tau^2)$ approximation to $w(t_{n+1})$, required for the third step of the method cannot be constructed in terms of w_n, w', and w''. In fact, in the explicit case it would follow that $\tilde{w}_{n+1} = \frac{9}{4}w'' - \frac{3}{4}w' - \frac{1}{2}w_n$ or, equivalently, $(\tilde{w}_{n+1} - w_n)/\tau = \frac{1}{4}F_n + \frac{3}{4}F'$. Since in the implicit case the variation of w' is $O(\tau^2)$ and the variation of w'' is $O(\tau^3)$, then the variation in $\tilde{w}_{n+1}$ is also $O(\tau^2)$, and it is no longer an $O(\tau^2)$ approximation to $w(t_{n+1})$.

The solution to the problem is to obtain $\tilde{w}_{n+1}$ from the following equation:

$$\frac{\tilde{w}_{n+1} - w_n}{\tau} = \frac{1}{4}F_n + \frac{3}{4}F' + \gamma L(\tilde{w}_{n+1} - \bar{w}_{n+1}) \tag{9}$$

Here, $\bar{w}_{n+1}$ is an $O(\tau)$ approximation to $w(t_{n+1})$, which may be taken as

$$\bar{w}_{n+1} = \tfrac{3}{2}(\alpha w' + (1 - \alpha)w'') - \tfrac{1}{2}w_n \tag{10}$$

Calculation of $\tilde{w}_{n+1}$ from (9) requires solution of a linear system with the matrix $I - \tau\gamma L$ (I is an identity matrix), and does not require additional evaluations of F. In (10), α is an arbitrary real parameter, but as will be shown later, the choice which allows economy of some run-time memory is

$$\alpha = \tfrac{3}{2} \tag{11}$$

The scheme (6)–(10) possesses a third-order accuracy irrespective of the values of α, γ, and of the operator L. In fact, different γ (and even different L) may be chosen for different steps of the scheme without a loss in the order of accuracy. For different γ, the scheme will have different implicit operators $I - \tau\gamma L$, so in the general case it would be more costly to precompute them, preinvert them and store them. Note that the scheme may be used in implicit ($L \neq 0$) mode as well as in explicit ($L \equiv 0$) modes.

3. STABILITY ANALYSIS

For a linear stability analysis we assume the operator of the system (1) to be linear and to coincide with the implicit operator, $F \equiv L$. Then, from (6)–(11) we derive the relation

$$w_{n+1} = R(\tau L)w_n \tag{12}$$

Here, the matrix-valued function R is called the *amplification matrix*, and the corresponding rational function $R(z)$ is the *stability function* of the scheme:

$$R(z) = (1-\gamma z)^{-4}[1-(4\gamma-1)z+(\gamma-\tfrac{1}{2})(6\gamma-1)z^2 - (4\gamma^3-6\gamma^2+2\gamma-\tfrac{1}{6})z^3+\gamma(\gamma-\tfrac{1}{2})(\gamma^2-2\gamma+\tfrac{1}{3})z^4] \tag{13}$$

For the A-stability of the scheme it is necessary $|R(z)| \leqslant 1$ for all z in the left semi-plane of a complex plane. A simple analysis shows that $\gamma \geqslant \frac{1}{3}$ is a necessary and sufficient condition for this. The optional requirement $R(z) \to 0$ for $z \to -\infty$ leads to $\gamma = \frac{1}{2}$ or $\gamma = 1 + (\frac{2}{3})^{1/2}$.

In numerical experiments with the Navier–Stokes equations we have found that the minimal possible γ produces the most accurate results. Stability conditions are similar for all $\gamma \geqslant \frac{1}{3}$. Thus, we recommend

$$\gamma = \tfrac{1}{3} \tag{14}$$

and all following considerations assume this value of γ.

4. LOCAL ERROR ESTIMATION AND TIME-STEP CONTROL

The scheme may be supplied with a local error estimation and time-step control algorithm based on the idea of embedded formulas [10]. After realization of all the steps of the scheme (6)–(9) we have at our disposal approximations to $w(t_{n+1})$ of two different orders:

$$w_{n+1} = w(t_{n+1}) + O(\tau^4) \quad \text{and} \quad \tilde{w}_{n+1} = w(t_{n+1}) + O(\tau^3) \tag{15}$$

Let $\|\cdot\|$ be a certain appropriate norm. The local error of integration $\varepsilon = \|w_{n+1} - w(t_{n+1})\|$ is $O(\tau^4)$, and at least for sufficiently small τ the inequality $\varepsilon < \mathrm{err}$ with

$$\mathrm{err} = \|w_{n+1} - \tilde{w}_{n+1}\| \tag{16}$$

will hold since $\mathrm{err} = O(\tau^3)$. Thus, with a certain portion of overestimation, err may be taken as an approximation to ε. For a given tolerance tol and supposing $\mathrm{err}(\tau) = C\tau^3$ the optimal time-step τ_{opt}, providing $\mathrm{err}(\tau_{\mathrm{opt}}) = \mathrm{tol}$, is determined by

$$\tau_{\mathrm{opt}} = \mathrm{fac}_{\mathrm{opt}} \cdot \tau, \quad \mathrm{fac}_{\mathrm{opt}} = (\mathrm{tol}/\mathrm{err})^{1/3} \tag{17}$$

If $\mathrm{fac}_{\mathrm{opt}}$ determined from (17) is too small, $\mathrm{fac}_{\mathrm{opt}} < \mathrm{fac}_{\mathrm{min}}$, with, say, $\mathrm{fac}_{\mathrm{min}} = 0.5$, then the complete step is considered as unsuccessful, and integration is repeated, starting with w_n (which is kept safe) with a smaller time-step τ_{new}, say, $\tau_{\mathrm{new}} = \mathrm{fac}_{\mathrm{min}} \cdot \tau$. Otherwise, the step is considered as successful, and time-step τ_{new} for the next step is set as

$$\tau_{\mathrm{new}} = \mathrm{fac} \cdot \tau, \quad \mathrm{fac} = \min\{\mathrm{fac}_{\mathrm{opt}}, \ \mathrm{fac}_{\mathrm{max}}\} \tag{18}$$

with, say, $\mathrm{fac}_{\mathrm{max}} = 1.5$.

4.1. Example: Van der Pole's equation

To illustrate the work of the time-step control algorithm we apply the scheme to Van der Pole's equation

$$\frac{\mathrm{d}x}{\mathrm{d}t} = y \equiv f_1(x, y)$$

$$\frac{\mathrm{d}y}{\mathrm{d}t} = \varepsilon(1 - x^2)y - x \equiv f_2(x, y)$$

For $\varepsilon \gg 1$ this system is stiff and requires an implicit method for numerical solution. For the implicit operator L we use the Jacobian $\partial(f_1, f_2)/\partial(x, y)$ computed at the initial time moment t_n for each time integration step $[t_n, t_{n+1}]$. Figure 1 presents the results for application

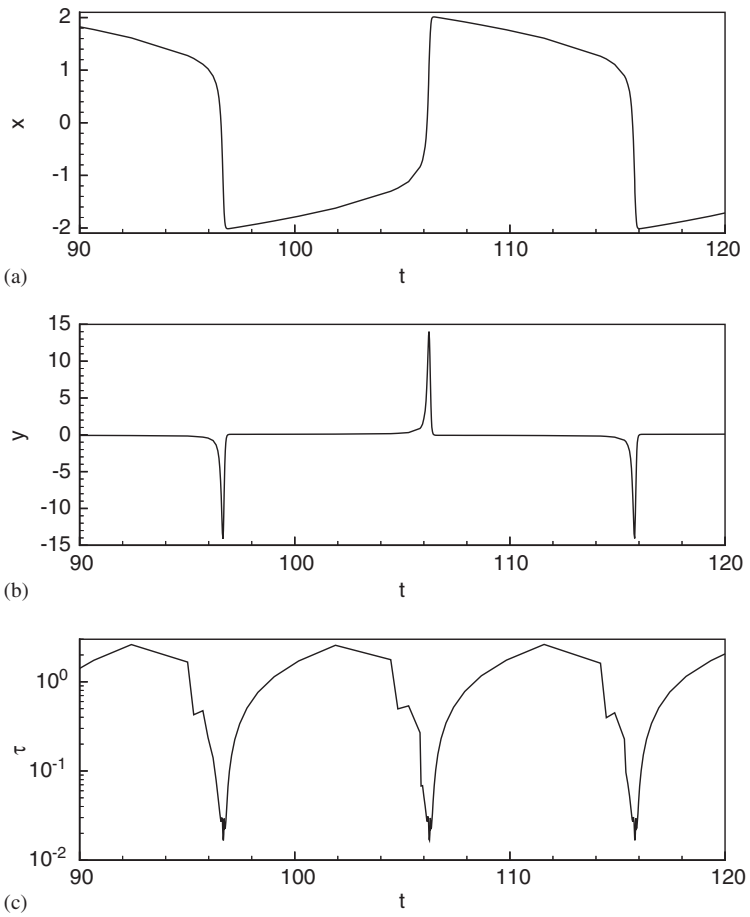

Figure 1. Solution of Van der Pole's equation: (a) $x(t)$; (b) $y(t)$; and (c) time history of time-step τ.

of the scheme (6)–(9) with $\mathrm{tol} = 10^{-3}$ and $\|w\| \equiv |x|$. In a limiting cycle corresponding to $\varepsilon = 10$, shown in the figure, the extended periods of slow variations in x alternate with abrupt sign changes. The behaviour of $\tau(t)$, shown in the Figure 1(c), reflects such a behaviour of the solution. Within a half-period of oscillation the time-step τ varies over two orders of magnitude. With the given tolerance $\mathrm{tol} = 10^{-3}$ integration over one period of oscillation requires about 60 time steps plus 4 unsuccessful steps.

5. APPLICATION TO NAVIER–STOKES EQUATIONS

The spatially discretized Navier–Stokes equations may be written in the following form:

$$\frac{\mathrm{d}w}{\mathrm{d}t} = H(t, w) - Gp \tag{19}$$

$$Dw + C_{\mathrm{bc}}(t) = 0 \tag{20}$$

Vectors $w(t)$, $p(t)$ represent the unknown velocities and pressures. G and D are the discrete gradient and divergence operators, respectively. H contains contributions from convection and viscous diffusion operators including contributions of the inhomogeneous boundary conditions. We suppose that boundary condition information is already incorporated into H, G, and D operators [8, 9]. Contributions of any inhomogeneous boundary conditions to the discretized continuity equation (20) is denoted by C_{bc}.

For a given velocity w, the pressure may be found after evaluation of H from the discrete Poisson equation which is a direct consequence of (19) and (20):

$$DGp = DH + \frac{\mathrm{d}C_{\mathrm{bc}}}{\mathrm{d}t} \tag{21}$$

After that the discretized Navier–Stokes equations are reduced to form (1) with

$$F = H - Gp \tag{22}$$

Now, scheme (6)–(9) may be directly applied for time advancement of the discretized Navier–Stokes equations. Starting from $w_n = w(t_n)$ and after completing all the steps, the final result w_{n+1} is an $O(\tau^3)$ approximation to $w(t_{n+1})$, which means that the local error $w_{n+1} - w(t_{n+1})$ is $O(\tau^4)$. In particular, supposing that the discrete incompressibility condition (20) was exactly satisfied for w_n for w_{n+1} we will have

$$Dw_{n+1} + C_{\mathrm{bc}}(t_{n+1}) = O(\tau^4) \tag{23}$$

The deficiency in the direct application of the scheme to the Navier–Stokes equations is that an error in the incompressibility condition accumulates during the repeatable process of time advancement, which may negatively affect the quality of the numerical solution. Fortunately, this deficiency may be easily improved by using a pressure splitting technique on the last step of the scheme. To show this, let us rename the final result of application (6)–(9) by u_{n+1} (instead of w_{n+1}). Then, the original formula for the last step may be written as

$$\frac{u_{n+1} - w_n}{\tau} = \frac{1}{4}F_n + \frac{3}{4}(H'' - Gp'') + \gamma L(u_{n+1} - \tilde{w}_{n+1}) \tag{24}$$

where p'' is a solution to the equation

$$DGp'' = DH'' + \frac{\mathrm{d}C_{\mathrm{bc}}(t + 2\tau/3)}{\mathrm{d}t} \tag{25}$$

Instead of using (24) we first calculate the auxiliary vector $\hat{w}_{n+1}$ from

$$\frac{\hat{w}_{n+1} - w_n}{\tau} = \frac{1}{4}F_n + \frac{3}{4}(H'' - Gp') + \gamma L(\hat{w}_{n+1} - \tilde{w}_{n+1}) \tag{26}$$

and then project it to the divergence-free field by subtracting an appropriate *pseudo-pressure* gradient Gq:

$$w_{n+1} = \hat{w}_{n+1} - Gq \tag{27}$$

$$Dw_{n+1} + C_{\mathrm{bc}}(t_{n+1}) = 0 \tag{28}$$

Now, the vector w_{n+1} satisfies the discrete incompressibility condition exactly. Let us show that w_{n+1} is another possible $O(\tau^3)$ approximation to $w(t_{n+1})$. It is sufficient for this to show that $w_{n+1} - u_{n+1} = O(\tau^4)$.

Comparison of (26) with (24) leads to the formula

$$(I - \gamma\tau L)(\hat{w}_{n+1} - u_{n+1}) = -\tfrac{3}{4}\tau G(p' - p'') \tag{29}$$

First, note that since $DGp' = DH' + \mathrm{d}C_{\mathrm{bc}}(t_n + 2\tau/3)/\mathrm{d}t$, $DGp'' = DH'' + \mathrm{d}C_{\mathrm{bc}}(t_n + 2\tau/3)/\mathrm{d}t$, and $H' - H'' = O(\tau^2)$ (this is a convenience of coincident abscissas), then

$$G(p' - p'') = O(\tau^2) \tag{30}$$

Two relations arise from (29) and (30)

$$\hat{w}_{n+1} - u_{n+1} = O(\tau^3) \tag{31}$$

$$\hat{w}_{n+1} - u_{n+1} = -\tfrac{3}{4}\tau G(p' - p'') + O(\tau^4) \tag{32}$$

Substitution of (27) into (29) produces the following:

$$(I - \gamma\tau L)(w_{n+1} - u_{n+1}) = -[Gq + \tfrac{3}{4}\tau G(p' - p'')] + \tau\gamma LGq \tag{33}$$

From (27), (28) the pseudo-pressure q satisfies the equation

$$DGq = D\hat{w}_{n+1} + C_{\mathrm{bc}}(t_{n+1}) \tag{34}$$

which may be rewritten as $DGq = Du_{n+1} + C_{\mathrm{bc}}(t_{n+1}) + D(\hat{w}_{n+1} - u_{n+1})$. Finally, taking into account that $Du_{n+1} + C_{\mathrm{bc}}(t_{n+1}) = O(\tau^4)$, we obtain $DGq = D(\hat{w}_{n+1} - u_{n+1}) + O(\tau^4)$. Now, from (31) it follows $DGq = O(\tau^3)$ which implies

$$Gq = O(\tau^3) \tag{35}$$

and from (32) we get

$$Gq + \tfrac{3}{4}\tau G(p' - p'') = O(\tau^4) \tag{36}$$

Hence, the rhs of (33) is $O(\tau^4)$ and, thus,

$$w_{n+1} - u_{n+1} = O(\tau^4) \tag{37}$$

It is useful to exclude F_n from the formula (7) for w'', to exclude F_n, F' from the formula (9) for $\tilde{w}_{n+1}$, and to exclude F_n from the formula (26) for $\hat{w}_{n+1}$. After that, the scheme takes the following compact form:

Step 1:

$$\begin{aligned} H_n &= H(t_n, w_n) \\ DGp_n &= DH_n + \mathrm{d}C_{\mathrm{bc}}(t_n)/\mathrm{d}t \\ (I - \gamma\tau L)(w' - w_n) &= \tfrac{2}{3}\tau(H_n - Gp_n) \end{aligned} \tag{38}$$

Step 2:

$$\begin{aligned} H' &= H(t_n + 2\tau/3, w') \\ DGp' &= DH' + \mathrm{d}C_{\mathrm{bc}}(t_n + 2\tau/3)/\mathrm{d}t \\ (I - \gamma\tau L)(w'' - \tfrac{3}{2}w' + \tfrac{1}{2}w_n) &= \tfrac{1}{3}\tau(H' - Gp') + w_n - w' \\ (I - \gamma\tau L)(\tilde{w}_{n+1} - \tfrac{3}{2}w'' + \tfrac{3}{4}w' - \tfrac{1}{4}w_n) &= \tfrac{3}{4}(w'' - w_n) \end{aligned} \tag{39}$$

Step 3:

$$\begin{aligned} H'' &= H(t_n + 2\tau/3, w'') \\ (I - \gamma\tau L)(\hat{w}_{n+1} - \tfrac{1}{2}\tilde{w}_{n+1} - \tfrac{3}{4}w'' + \tfrac{1}{4}w_n) &= \tfrac{3}{4}\tau(H'' - Gp') + \tfrac{5}{8}w_n + \tfrac{3}{8}w'' - \tilde{w}_{n+1} \\ DGq &= D\hat{w}_{n+1} + C_{\mathrm{bc}}(t_{n+1}) \\ w_{n+1} &= \hat{w}_{n+1} - Gq \end{aligned} \tag{40}$$

The benefit of choosing $\alpha = \frac{3}{2}$ (11) in (10) is that the last step formula (40) does not include vector w'. Thus, storage for only four velocity vectors plus one pressure vector is necessary to perform all the steps of the scheme. After calculation of w_{n+1} vectors $\tilde{w}_{n+1}$ and w_n are kept safe, so that the local error may be estimated by (16), and the integration may be repeated starting from t_n if necessary.

In the conclusion it is noted that the presented scheme is completely self-starting. Only an initial condition for the velocity w_n is needed to perform all the steps.

6. NUMERICAL EXAMPLE. FLOW IN A DRIVEN CAVITY

In this section, we present the verification of the constructed scheme considering unsteady laminar flows in a square cavity. The flows in a driven cavity have been used widely as a standard test case for evaluating the stability and accuracy of numerical methods for incompressible flow problems.

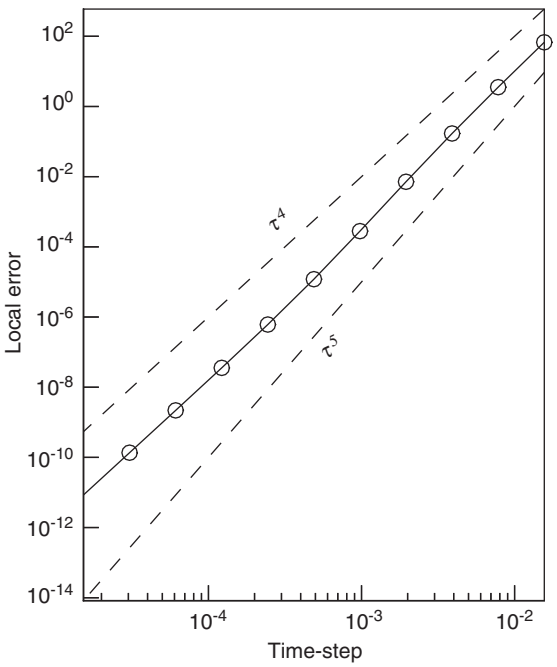

Figure 2. Local error as function of time-step τ.

The Navier–Stokes equations in a square domain ($0 \leqslant x \leqslant 1, 0 \leqslant y \leqslant 1$) are discretized on a 128×128 stretched staggered mesh. In each direction the mesh size in the neighbourhood of a boundary is about $\frac{1}{3}$ of that in the midplane. As is known, no *ad hoc* pressure boundary conditions are needed when using a staggered mesh. For solution of the discrete Poisson equation we use a direct method of cyclic reduction [11]. Only the viscous terms are treated implicitly using an approximate factorization method (i.e. operator L in (38)–(40) defined as

$$(I - \gamma\tau L) = \left(I - \frac{\gamma\tau}{Re}\frac{\partial^2}{\partial x^2}\right)\left(I - \frac{\gamma\tau}{Re}\frac{\partial^2}{\partial y^2}\right)$$

6.1. Estimation of the local error

In the first test case we consider the unsteady flow driven by the time-periodic movement of the upper wall and time-periodic suction through the upper wall:

$$u(x, y = 1) = \cos(\omega t), \quad v(x, y = 1) = 0.2\sin(2\pi x)\sin(\omega t), \quad \omega = 2\pi/10 \tag{41}$$

Hence, boundary conditions for the both tangential and normal velocities are inhomogeneous and unsteady. These artificial boundary conditions are chosen in order to demonstrate the ability of the scheme to properly handle the unsteady boundary conditions. Calculations are carried out at Reynolds number $Re = 100$ with zero initial conditions.

The goal is to show that the local error of time integration is $O(\tau^4)$. Starting from $t_0 \approx 40$ we perform one integration step with different τ. Because of the lack of an exact solution,

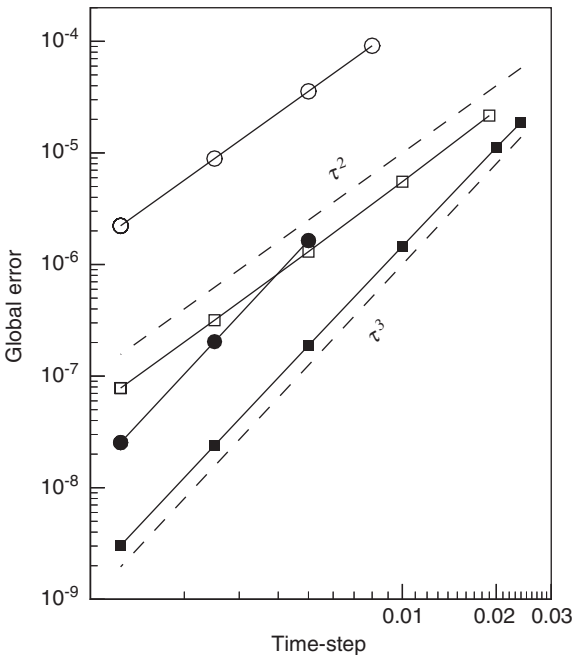

Figure 3. Global error as function of time-step τ. Closed squares, present scheme; open squares, semi-implicit Runge–Kutta scheme [4]; open circles, Adams–Bashforth/Crank–Nicolson scheme [1]; closed circles, semi-implicit one-step Adams–Bashforth/third-order backward Euler projection scheme [12]. The upper bound of τ for each scheme corresponds to the observed stability limit.

we compare the results of the implicit scheme with the results obtained with the use of the explicit scheme (2)–(4) which unquestionably approximates the exact solution within an $O(\tau^4)$ error. The maximum difference between these two solutions ε_{i-e} is shown in the Figure 2 as a function of the time-step τ. The $\sim\tau^4$ behaviour of the ε_{i-e} supports a third-order accuracy for the scheme.

6.2. *Stability and global accuracy analysis: comparison with other schemes*

In the second test case we consider the flow in a cavity driven by an impulsively started upper wall:

$$u(x, y=1)=1, \quad t\geqslant 0; \qquad u(x, y=1)=0, \quad t<0 \tag{42}$$

Calculations are carried out at Reynolds number $Re=1000$. At first, the equations are integrated from $t=0$ to 1 by an explicit fourth-order Runge–Kutta method. After that, starting from this 'initial' state the approximate solutions at $t=2$ are obtained with different τ and different methods. The results obtained using an explicit fourth-order accurate Runge–Kutta method with $\tau=10^{-4}$ are considered as 'exact', and the global errors corresponding to different methods and different $\tau>10^{-3}$ are evaluated by comparison with this 'exact' solution.

Besides, the present scheme the calculations were performed with several other semi-implicit schemes, namely: the semi-implicit Runge–Kutta scheme of [4], the Adams–Bashforth/Crank–Nicolson scheme of [1], and the scheme of [12]. The latter is a semi-implicit one-step Adams–Bashforth/third-order backward Euler projection scheme. There exists some uncertainty in the literature in handling the unsteady boundary conditions, and therefore the steady boundary condition case is chosen for the comparative analysis.

The results are summarized in Figure 3 where the global error as a function of the time-step τ is presented for each tested scheme. The maximum τ shown in Figure 3 for each scheme corresponds to its stability limit observed in calculation. The slopes of all the curves are consistent with the orders of accuracy: $\sim\tau^3$ for the present scheme and for the scheme [12], and $\sim\tau^2$ for the schemes [1, 4]. As was expected, the stability limit of the one-step methods for this high Reynolds number flow is considerably lower, than that of three-step Runge–Kutta schemes. On the whole, the present scheme looks preferable over second-order schemes both by accuracy and stability criteria. As for the scheme of [12], it looks advantageous over the present scheme with respect to accuracy, taking into account that it requires about three times less computations per time step. Probably, for low Reynolds number flows, when stability restriction of this scheme will be less pronounced, it may be preferable over the Runge–Kutta based schemes.

7. CONCLUSION

A semi-implicit Runge–Kutta scheme for the unsteady, incompressible Navier–Stokes equations with a third-order accuracy in time is devised. The higher order of accuracy is achieved due to one additional inversion of the implicit operator $I - \tau\gamma L$, which requires inversion of tridiagonal matrices when using an approximate factorization method. No additional solution of the pressure-Poisson equation or evaluation of the Navier–Stokes operator is needed. The temporal third-order accuracy of the scheme is proved analytically and ascertained by analysing both local and global errors in simulations of unsteady flows in a driven cavity. The constructed scheme promises to be an improvement over existing schemes for high Reynolds number flows.

REFERENCES

1. Kim J, Moin P. Application of a fractional-step method to incompressible Navier–Stokes equations. *Journal of Computational Physics* 1985; **59**:308–323.
2. Rai MM, Moin P. Direct simulations of turbulent flow using finite-difference schemes. *Journal of Computational Physics* 1991; **96**:15–53.
3. Spalart PR, Moser RD, Rogers M. Spectral methods for the Navier–Stokes equations with one infinite and two periodic directions. *Journal of Computational Physics* 1991; **96**:297–324.
4. Verzicco R, Orlandi P. A finite-difference scheme for the three-dimensional incompressible flows in cylindrical coordinates. *Journal of Computational Physics* 1996; **123**:402–414.
5. Nikitin NV. A spectral finite-difference method of calculating turbulent flows of an incompressible fluid in pipes and channels. *Computational Mathematics and Mathematical Physics* 1994; **34**:785–798.
6. Nikitin NV. Statistical characteristics of wall turbulence. *Fluid Dynamics* 1996; **31**:361–370.
7. Brown DL, Cortez R, Minion ML. Accurate projection methods for the incompressible Navier–Stokes equations. *Journal of Computational Physics* 2001; **168**:464–499.
8. Dukowicz JK, Dvinsky AS. Approximate factorization as a high order splitting for the implicit incompressible flow equations. *Journal of Computational Physics* 1992; **102**:336–347.
9. Perot JB. An analysis of the fractional step method. *Journal of Computational Physics* 1993; **108**:51–58.

10. Hairer E, Norsett SP, Wanner G. *Solving Ordinary Differential Equations. I. Nonstiff Problems*. Springer: Berlin, 1987.
11. Swarztrauber PN. A direct method for the discrete solutions of separable elliptic equations. *SIAM Journal of Numerical Analysis* 1974; **11**:1136–1150.
12. Botella O. On the solution of the Navier–Stokes equations using Chebyshev projection schemes with third-order accuracy in time. *Computers and Fluids* 1997; **26**:107–116.

